American Mineralogist, Volume 77, pages 848–856, 1992

Beryllophosphate chains in the structures of fransoletite, parafransoletite, and ehrleite and some general comments on beryllophosphate linkages

ANTHONY R. KAMPF

Mineralogy Section, Natural History Museum of Los Angeles County, 900 Exposition Boulevard,
Los Angeles, California 90007, U.S.A.

ABSTRACT

The crystal structures of the $Ca_3Be_2(PO_4)_2(PO_3OH)_2 \cdot 4H_2O$ dimorphs, fransoletite and parafransoletite, have been solved. The fransoletite structure was refined to residuals of $R = 0.088$ and $R_w = 0.109$ for 1161 observed reflections, and the parafransoletite structure to $R = 0.052$ and $R_w = 0.056$ for 1174 observed reflections. Fransoletite is monoclinic, $P2_1/a$, with $a = 7.348(1)$ Å, $b = 15.052(3)$ Å, $c = 7.068(1)$ Å, $\beta = 96.519(5)°$, and $Z = 2$. Parafransoletite is triclinic, $P\bar{1}$, with $a = 7.327(1)$ Å, $b = 7.696(1)$ Å, $c = 7.061(1)$ Å, $\alpha = 94.903(5)°$, $\beta = 96.820(5)°$, $\gamma = 101.865(5)°$, and $Z = 1$. The principal component in both structures is a tetrahedral chain parallel to [100] in which four-membered rings of alternating BeO_4 and PO_4 tetrahedra link to one another through the BeO_4 tetrahedra. The chains, in turn, are linked to one another by coordination to Ca and by H bonding. The only notable difference between the structures involves the placement of one of the two nonequivalent Ca atoms relative to the chains. These structures are closely related to the structure of ehrleite in which the same chains are also parallel to [100].

The four-membered tetrahedral ring is a recurring motif in beryllophosphate structures. Bond valence analysis provides a valuable tool in understanding the tetrahedral linkages in beryllophosphate structures. When used in conjunction with the Be/P ratio, it can place limitations on the possible linkages in unknown beryllophosphate structures.

INTRODUCTION

The beryllophosphates are few in number, but they are structurally intriguing. Only 19 beryllophosphate minerals are known, and the structures of 15 have been determined (including the two reported in this study). The structures of five synthetic zeolite-like beryllophosphates are also known (Harvey and Meier, 1989). All of these structures are based upon corner-sharing linkages of BeO_4 and PO_4 tetrahedra.

The O atoms shared only between Be and P tetrahedra receive Pauling bond valence sums of 1.75. The same bond valence sums are received by O atoms shared between Si and Al tetrahedra in aluminosilicates and between Si and B tetrahedra in borosilicates. It is therefore not surprising that some beryllophosphates are closely related to aluminosilicate or borosilicate structures (i.e., herderite ~ datolite, hurlbutite ~ danburite or anorthite, pahasapaite ~ zeolite ρ, tiptopite ~ basic cancrinite, synthetic beryllophosphate-P ~ pollucite).

Other beryllophosphate structures do not closely parallel silicate structures. One interesting example, ehrleite, $Ca_2ZnBe(PO_4)_2(PO_3OH) \cdot 4H_2O$, has a structure consisting of sheets of Be, P, and Zn tetrahedra in which Zn and partially occupied P tetrahedra link rigid chains of Be and P tetrahedra (Hawthorne and Grice, 1987). A rigid silicate or aluminosilicate chain of similar topology has not been noted.

Fransoletite, $H_2Ca_3Be_2(PO_4)_4 \cdot 4H_2O$, described by Peacor et al. (1983), and its dimorph parafransoletite, described by Kampf et al. (1992), exhibit nearly identical *a-c* lattice planes, which are also very similar to the *a-b* plane in ehrleite (see Table 1). This relationship in cell parameters suggests that the rigid tetrahedral chain in the ehrleite structure is also the basic structural unit in the fransoletite and parafransoletite structures.

The present study was undertaken to confirm the presence of the ehrleite beryllophosphate chain in fransoletite and parafransoletite, as well as to provide unequivocal evidence that fransoletite and parafransoletite are distinct species.

STRUCTURE DETERMINATIONS

Intensity data were measured using a Huber automated diffractometer with monochromatized Mo$K\alpha$ radiation and the $\theta/2\theta$ scan method. Data were corrected for Lorentz and polarization factors. All computations were carried out with the University of California, Los Angeles, crystallographic computing package. Scattering factors for neutral atoms and anomalous dispersion coefficients were taken from *International Tables for X-ray Crystallography* (Ibers and Hamilton, 1974).

Parafransoletite

Peacor et al. (1983) noted that they were unable to find a suitable crystal of fransoletite for crystal structure determination because of its pervasive mosaic texture. Con-

0003–004X/92/0708–0848$02.00

sequently, in the present study the solution of the parafransoletite was attempted first.

The crystal of parafransoletite for investigation was extracted from the holotype specimen (LACMNH 35696). The crystal was bounded by natural faces except for the broken surface, where it was separated from its matrix. The crystal dimensions were 0.10 × 0.02 × 0.06 mm, measured approximately along **a**, **b**, and **c**, respectively. The triclinic cell parameters provided in Table 1 were obtained by least-squares refinement of four-circle diffractometer data. A total of 2239 unique reflections was measured over one-half the complete sphere of reflection to a maximum 2θ of 60°. Of these, 1174 were considered observed with $I > 3\sigma(I)$. Because of the nonequidimensional shape of the crystal and its well-defined morphology, the data were corrected for absorption ($\mu_l = 15.7$ cm^{-1}).

The solution of the structure was straightforward by direct methods. Refining the positions and isotropic temperature factors of all non-H atoms yielded $R = 0.060$ and $R_w = 0.067$. Refinement using anisotropic temperature factors gave $R = 0.055$ and $R_w = 0.061$. A difference Fourier synthesis provided all five H atom positions. Although these positions could not be refined successfully, their incorporation into the structure lowered the R factors to $R = 0.052$ and $R_w = 0.056$ for the observed reflections ($R = 0.101$ and $R_w = 0.071$ for all reflections).

Fransoletite

The parafransoletite structure provided the basis for the derivation of a hypothetical structure for fransoletite. The superposition of the fransoletite cell on the parafransoletite structure such that their *a-b* planes and *a* axes coincided showed that the parafransoletite structure is compatible with the fransoletite cell and space group $P2_1/a$, the sole exception being the Ca at the special position 0,0,0. Even so, this Ca would have virtually identical surroundings in the fransoletite structure. In accordance with this model, fransoletite atomic coordinates were calculated using $x_f = x_p + y_p\cos\gamma_p$, $y_f = y_p/2$, $z_f = z_p$.

A fransoletite crystal from the type specimen (NMNH 149607) was carefully broken under acetone. A cleavage fragment 0.12 × 0.06 × 0.09 mm, exhibiting uniform extinction under crossed polars in all orientations, was chosen for structure analysis. It was hoped that the small crystal size would serve to minimize the mosaic effect noted by Peacor et al. (1983), an assumption supported by the uniform extinction.

The monoclinic cell parameters for fransoletite (Table 1), obtained by least-squares refinement of four-circle diffractometer data, agree closely with those reported by Peacor et al. (1983). Omega peak scans for numerous reflections were examined and were deemed acceptably sharp and symmetrical. A total of 4436 reflections allowed by the space group was measured over one-half the sphere of reflection to a maximum 2θ of 60°. Of these, 2203 met the $I > 3\sigma(I)$ criterion for being considered observed. Averaging of equivalent reflections resulted in 1161 independent reflections with an agreement index of 0.030. Because of the crystal's small size, relatively equidimensional aspect, and low linear absorption coefficient ($\mu_l = 15.5$ cm^{-1}), an absorption correction was not immediately applied.

Table 1. Cell parameters for parafransoletite, fransoletite, and ehrleite

	Fransoletite	Parafransoletite	Ehrleite*
Space group	$P2_1/a$	$P\bar{1}$	$P\bar{1}$
a (Å)	7.3482(13)	7.3275(13)	7.130(4)
b (Å)	15.0522(28)	7.6959(13)	7.430(4)
c (Å)	7.0685(13)	7.0606(13)	12.479(9)
α (°)	—	94.903(5)	94.31(5)
β (°)	96.519(6)	96.820(5)	102.07(4)
γ (°)	—	101.865(5)	82.65(4)
V (Å^3)	776.8(2)	384.6(1)	640.3(6)
Z	2	1	1

* Data from Hawthorne and Grice (1987).

The refinement of the fransoletite structure by using the atomic coordinates calculated for the hypothetical fransoletite structure, as noted above, was successful. Refining the positions and isotropic temperature factors of all non-H atoms yielded $R = 0.097$ and $R_w = 0.120$. One O atom, O4, attained a somewhat low temperature factor of 0.5 Å^2. Refinement using anisotropic temperature factors yielded $R = 0.087$ and $R_w = 0.108$. The β_{33} coefficient for O4 became slightly nonpositive, but all other anisotropic temperature factors were reasonable. Application of an absorption correction at this point by means of an approximated morphology yielded slightly higher R values and failed to improve the temperature factor of O4. An absorption correction was, therefore, not subsequently employed.

Comparison of O4 bond distances in fransoletite with those in parafransoletite (Table 2) and bond valence sums for P1 and Be in the two minerals (Tables 3a, 3b) suggests that in fransoletite the distance Pl-O4 is too long and Be-O4 too short. Examination of the Fourier map showed the O4 peak to be abnormally elongated approximately parallel to the **a** axis. Constraining the x coordinate of O4 to 0.813 rather than 0.803 (its refined value) yielded appropriate distances and bond valence sums; however, the temperature factor increased only slightly, and the R values for both isotropic and anisotropic refinements increased by 0.002. The O4 site returned to its previous position when this positional constraint was removed. Refinement in space group $P\bar{1}$ yielded nearly identical results.

A difference Fourier synthesis showed many small peaks. Two of these approximated the predicted positions for H_{OH} and H2a; however, peaks in the general vicinity expected for H1a, H1b, and H2b did not correspond closely with those in parafransoletite. The latter three positions also yielded abnormal O-H distances and O-H···O angles (Table 4). When all five H positions were incorporated into the structure, the refinement improved to R

TABLE 2. Selected bond lengths (Å) in fransoletite and parafransoletite

	Fransoletite	Parafransoletite
Ca1-O1	2.463(10)	2.467(5)
-O3	2.417(10)	2.430(5)
-O5	2.318(10)	2.316(5)
-O5′	2.539(9)	2.523(5)
-O6	2.482(10)	2.476(5)
-OW1	2.542(10)	2.461(5)
-OW2	2.509(10)	2.527(5)
Average	2.467	2.457
Ca2-O1	2.430(10) × 2	2.450(5) × 2
-O7	2.293(9) × 2	2.303(5) × 2
-OW2	2.460(10) × 2	2.462(5) × 2
Average	2.394	2.405
P1-O1	1.523(9)	1.518(5)
-O2 = OH	1.581(10)	1.571(5)
-O3	1.538(10)	1.533(5)
-O4	1.556(9)	1.514(5)
Average	1.550	1.534
P2-O5	1.524(10)	1.514(5)
-O6	1.550(10)	1.549(5)
-O7	1.534(10)	1.537(5)
-O8	1.534(9)	1.540(5)
Average	1.536	1.535
Be-O3	1.629(20)	1.644(9)
-O4	1.565(18)	1.634(9)
-O6	1.610(19)	1.601(9)
-O8	1.640(20)	1.597(9)
Average	1.611	1.619

= 0.085 and R_w = 0.103. Nevertheless, the relatively high R factors for the refinement and the aforementioned considerations indicate that all five H atoms in the fransoletite structure should be considered poorly located.

During the final refinement cycles an isotropic temperature factor was employed for O4 and H atom positions were not included. This yielded R = 0.088 and R_w = 0.109 for the observed reflections and R = 0.137 and R_w = 0.120 for all reflections. The higher R values obtained for fransoletite as compared to parafransoletite, the difficulty in refining the position and temperature factors for O4, and the difficulty in locating the H atoms are probably attributable to lesser quality data for fransoletite (possibly resulting from its mosaic nature) rather than to a subtle form of twinning or disorder.

The coordinates and isotropic temperature factors for both fransoletite and parafransoletite are listed in Table 5, anisotropic temperature factors in Tables 6a and 6b,[1] the observed and calculated structure factors in Tables 7a and 7b, metal-O distances in Table 2, H bond distances and angles in Table 4, polyhedral O-O distances and O-M-O angles in Table 8, and empirical bond valences in Tables 3a and 3b.

TABLE 3A. Empirical bond valences* in fransoletite

	P1	P2	Be	Ca1	Ca2	H_{OH}	H1a	H1b	H2a	H2b	Σv_a
O1	1.24			0.26	0.29(×2↓)						1.79
O2	1.06					0.80					1.86
O3	1.20		0.51	0.30							2.01
O4	1.14		0.61						0.18		1.93
O5		1.24		0.39 + 0.21							1.84
O6		1.16	0.54	0.25							1.95
O7		1.21			0.41(×2↓)	0.20		0.17			1.99
O8		1.21	0.50				0.16				1.87
OW1				0.21			0.84	0.83		0.17	2.05
OW2				0.23	0.26(×2↓)				0.82	0.83	2.14
Σv_c	4.64	4.82	2.16	1.84	1.92	1.00	1.00	1.00	1.00	1.00	

* Based upon Brese and O'Keeffe (1991), except for H bonds, which are based upon the curve of Brown and Altermatt (1985) applied to the corresponding O-O distances.

TABLE 3B. Empirical bond valences* in parafransoletite

	P1	P2	Be	Ca1	Ca2	H_{OH}	H1a	H1b	H2a	H2b	Σv_a
O1	1.26			0.26	0.27(×2↓)						1.79
O2	1.09					0.80					1.89
O3	1.21		0.49	0.29							1.99
O4	1.28		0.50						0.18		1.96
O5		1.28		0.39 + 0.22							1.89
O6		1.16	0.55	0.25							1.96
O7		1.20			0.40(×2↓)	0.20		0.18			1.98
O8		1.19	0.56				0.18				1.93
OW1				0.26			0.82	0.82		0.16	2.06
OW2				0.22	0.26(×2↓)				0.82	0.84	2.14
Σv_c	4.84	4.83	2.10	1.89	1.86	1.00	1.00	1.00	1.00	1.00	

* Based upon Brese and O'Keeffe (1991), except for H bonds, which are based upon the curve of Brown and Altermatt (1985) applied to the corresponding O-O distances.

---

[1] A copy of Tables 6a, 6b, 7a, and 7b may be ordered as Document AM-92-499 from the Business Office, Mineralogical Society of America, 1130 Seventeenth Street NW, Suite 330, Washington, DC 20036, U.S.A. Please remit $5.00 in advance for the microfiche.

TABLE 4. H bond distances (Å) and angles (°)

	Fransoletite*	Parafransoletite
O2-O7	2.754(13)	2.744(7)
O2-H$_{OH}$	0.914	0.825
O7···H$_{OH}$	1.862	1.948
∠O-H-O	164.4	162.2
OW1-O8	2.871(12)	2.811(6)
OW1-H1a	0.837	0.926
O8···H1a	2.494	2.019
∠O-H-O	108.4	142.4
OW1-O7	2.845(13)	2.824(7)
OW1-H1b	0.736	0.902
O7···H1b	2.136	2.115
∠O-H-O	162.2	134.7
OW2-O4	2.794(12)	2.824(6)
OW2-H2a	0.787	0.848
O4···H2a	2.007	2.002
∠O-H-O	176.8	162.9
OW2-OW1	2.856(13)	2.884(7)
OW2- H2b	1.009	0.945
OW1···H2b	2.267	2.023
∠O-H-O	115.9	150.7

* The H positions in fransoletite are poorly determined; only the H$_{OH}$ and H2a positions yield reasonable distances and angles.

STRUCTURE DESCRIPTIONS AND RELATIONSHIPS TO EHRLEITE

Figure 1 depicts the structures of fransoletite and parafransoletite projected along [001] and that of ehrleite projected along [010]. The same distinctive Be-P tetrahedral chain is parallel to the **a** axis in all three structures. The resemblance extends also to the Ca atoms, which bond to the chains and link them together. This is manifested by the very similar *c* axis lengths of fransoletite and parafransoletite and the *b* axis length of ehrleite. To facilitate comparisons of the three structures, the atoms in fransoletite and parafransoletite are labeled to correspond to atoms in the ehrleite structure (Hawthorne and Grice, 1987).

The structures differ principally in the linkage between chains in the [010] direction in fransoletite and parafransoletite and in the [001] direction in ehrleite. The fransoletite and parafransoletite structures differ with respect to the relative placement of Ca2 on either side of the chain, which in turn leads to a translation in adjacent chains relative to one another. The chain-Ca2 configuration in ehrleite matches that in parafransoletite, such that Ca2 atoms in ehrleite can be joined as shown in Figure 1 to approximate the unit cell of parafransoletite. Thus removal of the Zn, P3, and P4 tetrahedra that link the chains in ehrleite followed by collapse of the structure in the [001] direction would yield the parafransoletite structure.

The close relationship between the structures is further seen in Figure 2, in which projections along [100], the chain direction, are compared. The arrangement of Ca in layers between the chains is evident in this projection.

Tetrahedral chains

The tetrahedral chains consist of four-membered rings of alternating Be and P tetrahedra (Fig. 3), which in turn are linked to one another by sharing the Be tetrahedra of the rings. The O-P-O and O-Be-O angles in all tetrahedra in fransoletite and parafransoletite are within the normal range. The P-O and Be-O bonds are all within the ranges observed in other structures; however, two points deserve special comment.

The P1-O2 distance in both fransoletite and parafransoletite is significantly longer than the other P-O bonds. The bond valence sums for O2 (Tables 3a, 3b) indicate that it is an OH group in both structures.

TABLE 5. Positional and equivalent isotropic thermal parameters in fransoletite and parafransoletite

	Fransoletite				Parafransoletite			
Atom	*x*	*y*	*z*	B_{eq} (Å^2)	*x*	*y*	*z*	B_{eq} (Å^2)
Ca1	0.6365(4)	0.1968(2)	0.9508(4)	0.77(4)	0.7103(2)	0.3915(2)	0.9772(2)	1.00(3)
Ca2	0	0	0	1.24(7)	0	0	0	1.22(4)
P1	0.9741(4)	0.1514(2)	0.6470(4)	0.54(5)	0.0430(2)	0.3020(2)	0.6843(2)	0.75(3)
P2	0.2903(4)	0.1520(2)	0.2322(4)	0.46(5)	0.3563(2)	0.3020(2)	0.2675(2)	0.76(3)
Be	0.6328(25)	0.2106(11)	0.4481(25)	0.6(2)	0.7334(12)	0.4197(11)	0.4862(12)	0.7(1)
O1	0.9272(12)	0.1430(7)	0.8506(12)	0.9(1)	0.9881(6)	0.2891(6)	0.8841(7)	1.2(1)
O2 = OH	0.0993(13)	0.0690(6)	0.6114(13)	1.1(2)	0.1335(6)	0.1384(6)	0.6353(7)	1.3(1)
O3	0.0905(13)	0.2359(6)	0.6386(13)	1.0(2)	0.1950(6)	0.4733(6)	0.6925(6)	1.0(1)
O4	0.8028(11)	0.1486(6)	0.4959(12)	0.5(1)	0.8779(6)	0.2872(6)	0.5286(6)	0.8(1)
O5	0.3451(13)	0.1711(6)	0.0346(13)	1.0(2)	0.4137(6)	0.3307(6)	0.0716(6)	1.2(1)
O6	0.1561(13)	0.2284(7)	0.2652(13)	1.1(2)	0.2592(6)	0.4576(6)	0.3170(6)	0.9(1)
O7	0.1886(13)	0.0635(6)	0.2436(13)	1.0(2)	0.2159(6)	0.1234(6)	0.2659(7)	1.2(1)
O8	0.4558(12)	0.1465(6)	0.3850(12)	0.8(1)	0.5252(6)	0.3028(6)	0.4202(7)	1.1(1)
OW1	0.5234(13)	0.0631(6)	0.7515(13)	1.1(2)	0.5521(7)	0.1270(6)	0.7520(7)	1.4(1)
OW2	0.7390(13)	0.0625(7)	0.1445(13)	1.2(2)	0.7603(6)	0.1256(6)	0.1473(7)	1.2(1)
H$_{OH}$	0.108	0.063	0.484	3.2	0.133	0.129	0.518	3.2
H1a	0.425	0.088	0.710	3.2	0.496	0.143	0.632	3.2
H1b	0.581	0.023	0.756	3.2	0.656	0.098	0.713	3.2
H2a	0.761	0.086	0.244	3.2	0.817	0.183	0.253	3.2
H2b	0.718	0.997	0.121	3.2	0.635	0.067	0.154	3.2

Note: Estimated standard deviations are in parentheses. H positions were approximated from difference Fourier maps; their positions and thermal parameters were not refined. Fransoletite coordinates can be approximately derived from the parafransoletite coordinates as follows: $x_f = x_p + y_p \cos \gamma_p$, $y_f = y_p/2$, $z_f = z_p$.

Table 8. Polyhedral edges and angles in fransoletite and parafransoletite

	Fransoletite		Parafransoletite		
	O-O (Å)	O-M-O (°)	O-O (Å)	O-M-O (°)	
Ca1 polyhedron*					
O1-O3	3.294	84.9	3.151	83.2	O3-O5
O1-O5′	3.172	78.7	2.968	75.5	O5-O5′
O1-OW2	2.889	71.1	2.845	69.4	O1-OW2
O1-OW1	3.205	79.6	3.176	80.3	O1-OW1
O3-O5	3.767	105.4	3.887	105.1	O1-O3
O3-O5′	3.331	84.4	3.338	84.7	O3-O5′
O3-OW1	3.182	79.8	3.133	78.4	O3-OW2
O5-O6	3.054	78.9	3.227	81.5	O1-O6
O5′-O6	2.418	57.6	2.423	58.0	O5′-O6
O5-OW1	2.993	75.9	3.028	78.6	O5-OW1
O5-OW2	3.338	87.4	3.271	84.8	O5-OW2
O6-OW2	3.335	83.9	3.313	84.3	O6-OW1
OW2-OW1	3.038	73.9	3.020	74.5	OW2-OW1
Average	3.155	80.1	3.137	79.9	
Ca2 octahedron					
O1-O7 ×2	3.271	87.6	3.245	86.1	
O1-O7 ×2	3.410	92.4	3.474	93.9	
O1-OW2 ×2	2.889	72.4	2.845	70.8	
O1-OW2 ×2	3.945	107.6	4.004	109.2	
O7-OW2 ×2	3.426	92.2	3.394	90.8	
O7-OW2 ×2	3.299	87.8	3.348	89.2	
Average	3.373	90.0	3.385	90.0	
P1 tetrahedron					
O1-O2	2.487	106.5	2.484	107.1	
O1-O3	2.460	107.0	2.464	107.7	
O1-O4	2.571	113.2	2.542	113.9	
O2-O3	2.521	107.8	2.512	108.1	
O2-O4	2.539	108.0	2.466	106.1	
O3-O4	2.594	114.0	2.549	113.6	
Average	2.529	109.4	2.503	109.4	
P2 tetrahedron					
O5-O6	2.418	103.7	2.423	104.5	
O5-O7	2.552	113.1	2.534	112.4	
O5-O8	2.545	112.6	2.541	112.6	
O6-O7	2.500	108.3	2.515	109.2	
O6-O8	2.581	113.6	2.552	111.4	
O7-O8	2.443	105.6	2.470	106.8	
Average	2.507	109.5	2.506	109.5	
Be tetrahedron					
O3-O4	2.614	109.8	2.611	105.6	
O3-O6	2.738	115.4	2.744	115.5	
O3-O8	2.631	107.2	2.641	109.2	
O4-O6	2.617	111.0	2.600	107.0	
O4-O8	2.581	107.3	2.637	109.4	
O6-O8	2.591	105.7	2.619	110.0	
Average	2.629	109.4	2.642	109.5	

Note: Estimated standard deviations for fransoletite are O-O = 0.013 Å, O-Ca-O = 0.3°, O-P-O = 0.5°, O-Be-O = 1.0°; for parafransoletite they are O-O = 0.006 Å, O-Ca-O = 0.2°, O-P-O = 0.3°, O-Be-O = 0.5°.

* Differing space group generators for fransoletite and parafransoletite in some cases require that different O-O pairs represent geometrically equivalent edges in the Ca1 coordination polyhedron. These have been arranged accordingly to facilitate comparisons.

The greater than normal P1-O4 distance and smaller than normal Be-O4 distance in fransoletite cannot be explained using bond valence considerations. As mentioned earlier, the position of the O4 atom in fransoletite should therefore be considered suspect. The very low bond valence sum for P1 and the somewhat high sum for Be in fransoletite provide further support for this conclusion. No structural reason could be found for the abnormal refined centroid of O4.

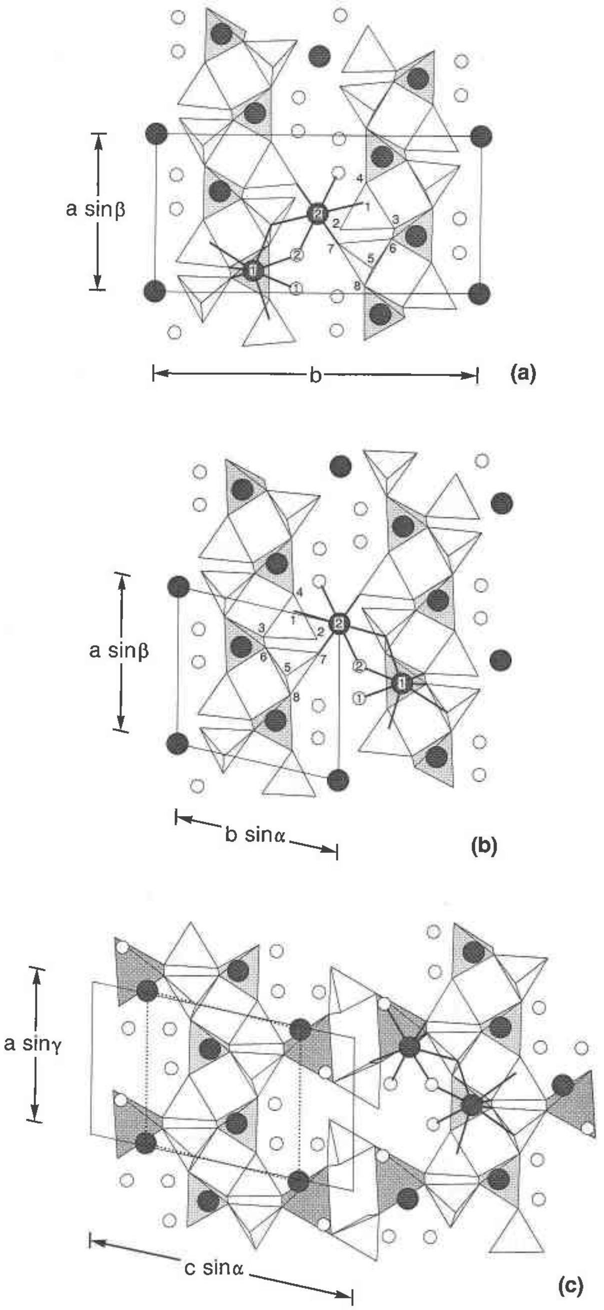

Fig. 1. The structures of (**a**) fransoletite and (**b**) parafransoletite, both projected along [001], and (**c**) ehrleite projected along [010]. Darkly shaded circles are Ca atoms, unshaded circles are H_2O O atoms. In **a** and **b**, number labels are shown for Ca atoms (1 and 2), H_2O O atoms (1 and 2), and tetrahedral O atoms (1–8). Bonds surrounding one Ca1 and one Ca2 atom in each structure are shown. The BeO_4 tetrahedra are located directly beneath Ca1 atoms. The Ca2 atoms in ehrleite partially overlap the ZnO_4 tetrahedra. A solid line outlines the unit cell in each structure. The dotted outline on the ehrleite drawing approximates the parafransoletite cell.

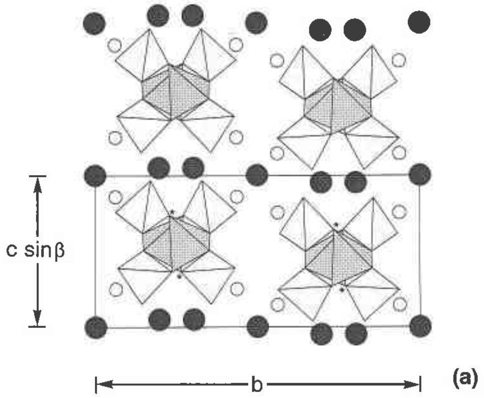

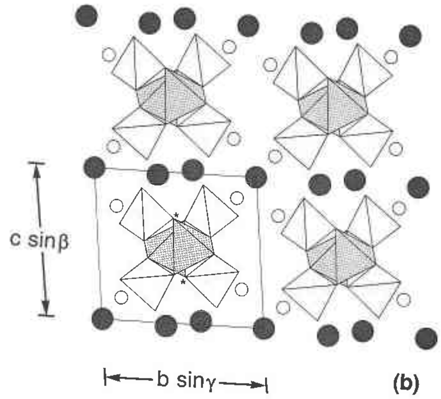

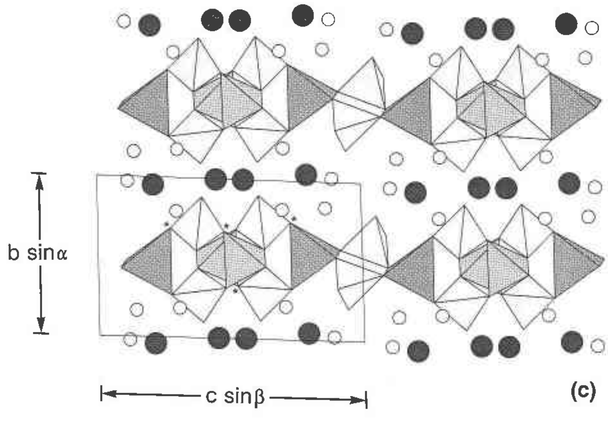

Fig. 2. The structures of (**a**) fransoletite, (**b**) parafransoletite, and (**c**) ehrleite, all projected down [100]. The BeO_4 tetrahedra overlap one another. Asterisks indicate apparent tetrahedral joins; the tetrahedra are actually attached to corresponding tetrahedra above or below.

Ca coordination

The Ca1 atoms located directly above the Be tetrahedra in the projections shown in Figure 1 are sevenfold coordinated in fransoletite and parafransoletite and eightfold coordinated in ehrleite. Each links to one O1, O5, and O6 in one chain, one O3 and O5 in a second chain, and two H_2O O atoms, OW1 and OW2. In ehrleite the eighth bond is to an O1 in the second chain. The Ca1-O distances range from 2.32 to 2.54 Å in fransoletite and parafransoletite and 2.39 to 2.58 Å in ehrleite. The difference in coordination is due to slight differences in the relative inclinations of chains on either side of Ca1 (Fig. 2), which increases the second Ca1-O1 distance to 2.90 Å in fransoletite and 2.95 Å in parafransoletite. (These latter distances actually are within the range for Ca-O bond distances, 2.25–2.96 Å, given by Baur, 1970.)

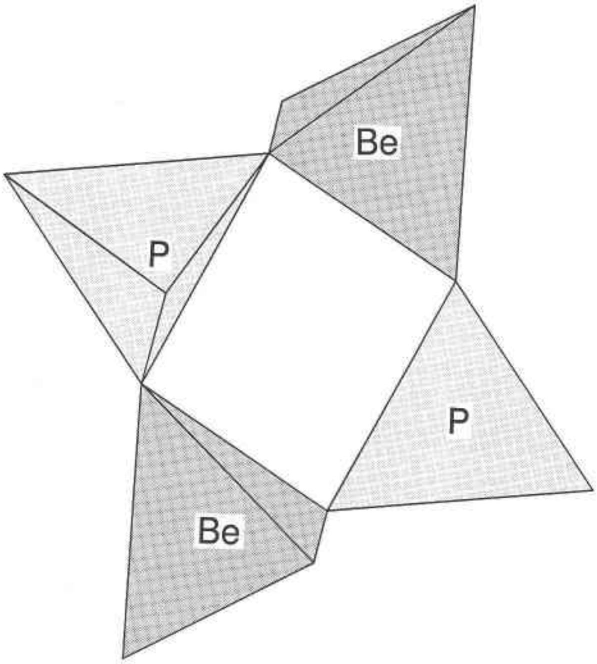

Fig. 3. The four-membered ring of alternating BeO_4 and PO_4 tetrahedra found in the structures of numerous beryllophosphates.

An intriguing aspect of the distinct chain to Ca2 configurations in fransoletite and parafransoletite is that they lead to virtually identical Ca2 coordinations. The Ca2 atoms are located at the origin (center of symmetry) in fransoletite and parafransoletite and exhibit sixfold coordination in the form of a distorted octahedron. The Ca2-O bond lengths and O-Ca2-O angles are quite similar in the two structures. Each Ca2 bonds to O atoms in four different chains (two O1 and two O7 atoms), as well as to two OW2 atoms. Other than H bonds, the only linkage between chains in the **b** direction in fransoletite and parafransoletite is by these Ca2-O bonds.

In ehrleite Ca2 is sevenfold coordinated but exhibits a similar relationship to the chains, as seen in Figures 1 and 2. Each Ca2 in ehrleite bonds to O1 and O2 in one chain and to O7 in a second chain, as well as to one OW2. The three other ligands are two H_2O molecules and a nonchain phosphate O atom, none of which corresponds to entities in the fransoletite or parafransoletite structures. Again, the difference in coordination is due to differences in the relative inclinations of the chains, which yields much greater Ca2-O2 distances of 3.10 Å in fransoletite and 3.06 Å in parafransoletite.

As Tables 3a and 3b indicate, the empirical bond valence sums for Ca1 and Ca2 in both fransoletite and parafransoletite are significantly smaller than ideal. Including the two distant O1 atoms in the coordination of Ca1 and the two distant O2 atoms in the coordination of Ca2 improves the bond valence sums for all of the atoms involved (fransoletite: Ca1 1.84 → 1.92, Ca2 1.92 → 2.01, O1 1.79 → 1.87, O2 1.86 → 1.91; parafransoletite: Ca1 1.89 → 1.96, Ca2 1.86 1.86 → 1.96, O1 1.79 → 1.86, O2 1.89 → 1.94 vu). It may, therefore, be more appropriate to refer to Ca1 as having 7 + 1 coordination and Ca2 as having 6 + 2 coordination in fransoletite and parafransoletite.

OH, H_2O, and H bonding

Atoms OW1 and OW2 are situated in approximately the same positions relative to the chains in all three structures. Atom OW1 is bonded to one Ca1, and OW2 is shared by one Ca1 and one Ca2. Atom O2 is an OH group in both fransoletite and parafransoletite, and it is bonded only to P1. In ehrleite this is an O atom shared by P1 and Zn.

The quality of the data was sufficient to locate all H atoms approximately only for parafransoletite; however, the close parallel between the fransoletite and parafransoletite structures suggests that they possess essentially identical H bonding schemes. Five H bonds were noted: O2-H···O7, OW1-H1a···O8, OW1-H1b···O7, OW2-H2a···O4, and OW2-H2b···OW1. The H bonds are shown for the parafransoletite structure in Figure 4. H bond distances and angles are given in Table 2; however, Brown and Altermatt (1985) noted that X-ray diffraction studies usually show H atom centroids that are closer to the donor anion than they actually are. This situation arises because electrons, not nuclei, scatter X-rays. They propose an O-H distance of 0.95 Å. Because of the relatively large uncertainty in the location of H positions in parafransoletite and the difficulty in locating them at all in fransoletite, the bond valences for H bonds in these two structures given in Tables 3a and 3b are based upon the corresponding O-O distances utilizing the curve of Brown and Altermatt (1985).

Hawthorne and Grice (1987) proposed a H bonding scheme in ehrleite based upon bond valence considerations and geometry. Only two similarities with the fransoletite-parafransoletite scheme are evident, i.e., OW1-H1a···O8 and OW2-H2a···O4. A notable difference is that the O2-H···O7 bond in fransoletite and parafransoletite is replaced by a ZnO_4 tetrahedral edge in ehrleite.

CORRELATIONS AMONG BERYLLOPHOSPHATE STRUCTURES

Chains of the type found in the structures of fransoletite, parafransoletite, and ehrleite have not been reported in other beryllophosphates or in any alumino- or borosilicates. However, four-membered rings of alternating Be and P tetrahedra such as those constituting the chains in these three structures (Fig. 3) are a recurring motif in beryllophosphate structures. They make up portions of the tetrahedral frameworks in beryllonite (Giuseppetti and Tadini, 1973), hurlbutite (Lindbloom et al., 1974), pahasapaite (Rouse et al., 1989), tiptopite (Peacor et al., 1987), weinebeneite (Walter, 1991), and the five synthetic zeolite-like beryllophosphates described by Harvey and Meier (1989); the tetrahedral sheets in herderite and hydroxylherderite (Lager and Gibbs, 1974); and the tetrahedral chains in roscherite (Fanfani et al., 1977) and zanazziite (Fanfani et al., 1975). [Leavens et al. (1990) described zanazziite and showed that Fanfani et al. (1975) actually worked on zanazziite rather than what they referred to as "monoclinic roscherite."] The roscherite and zanazziite chains resemble the chains found in fransoletite, parafransoletite, and ehrleite. The four-membered rings in all five minerals possess very similar geometry; however, in roscherite and zanazziite the rings are joined into chains by sharing the vertices of additional bridging phosphate tetrahedra (compare Fig. 3 in Fanfani et al., 1975).

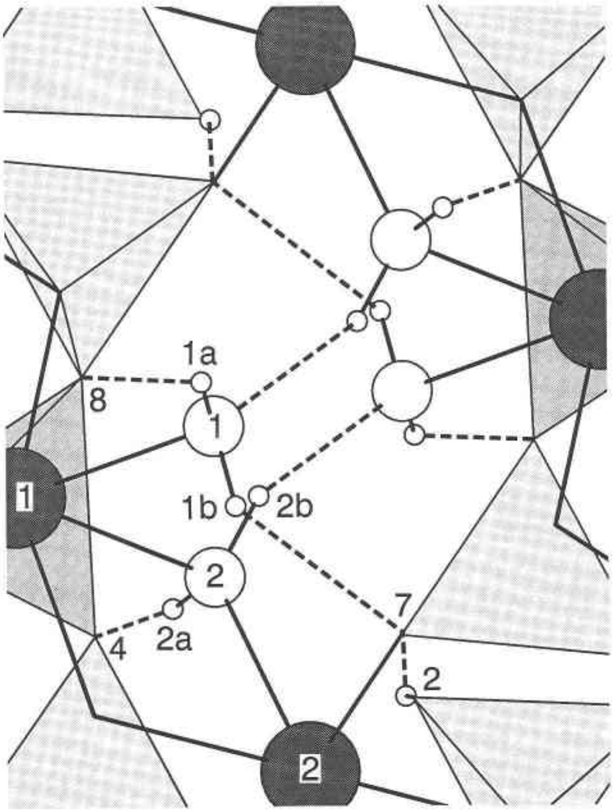

Fig. 4. Bonding in a portion of the parafransoletite structure projected along [001]. Darkly shaded circles are Ca atoms, large unshaded circles are H_2O O atoms, and small unshaded circles are H atoms. The Ca-O and O-H bonds are shown as solid lines; H bonds are shown as dashed lines.

Four-membered rings are absent from the beryllophosphate linkages in only three known structures: the framework structure of babefphite (Simonov et al., 1980), the chain structure of väyrynenite (Mrose and Appleman,

TABLE 9. Be/P ratios in beryllophosphates

Structure*	Beryllophosphate	Formula	Be/P
Framework	weinebeneite	$CaBe_3(PO_4)_2(OH)_2 \cdot 4H_2O$	1/0.67
	babefphite	$BaBePO_4(F,O)$	1/1
	beryllonite	$NaBePO_4$	1/1
	hurlbutite	$CaBe_2(PO_4)_2$	1/1
	pahasapaite	$Li_8(Ca,Li,K)_{10.5}Be_{24}(PO_4)_{24} \cdot 38H_2O$	1/1
	tiptopite	$K_2(Li,Na,Ca)_6Be_6(PO_4)_6(OH)_2 \cdot 1.3H_2O$	1/1
	beryllophosphate-R**	$Li_3Be_3(PO_4)_3 \cdot 5H_2O$	1/1
	beryllophosphate-G**	$Na_4Be_4(PO_4)_4 \cdot 5H_2O$	1/1
	beryllophosphate-E**	$KBePO_4 \cdot H_2O$	1/1
	beryllophosphate-P**	$Cs_2Be_3(PO_4)_3H$	1/1
	beryllophosphate-H**	$Na_7K_7Be_{14}(PO_4)_{14} \cdot 20H_2O$	1/1
Sheet	herderite	$CaBePO_4(F,OH)$	1/1
	hydroxylherderite	$CaBePO_4(OH)$	1/1
Chain	väyrynenite	$MnBePO_4(OH,F)$	1/1
	roscherite	$Ca_2(Fe,Mg)_5Be_4(PO_4)_6(OH)_4 \cdot 6H_2O$	1/1.5
	zanazziite	$Ca_2(Mg,Fe)_5Be_4(PO_4)_6(OH)_4 \cdot 6H_2O$	1/1.5
	fransoletite	$Ca_3Be_2(PO_4)_2(PO_3OH)_2 \cdot 4H_2O$	1/2
	parafransoletite	$Ca_3Be_2(PO_4)_2(PO_3OH)_2 \cdot 4H_2O$	1/2
	ehrleite	$Ca_2ZnBe(PO_4)_2(PO_3OH) \cdot 4H_2O$	1/3
Cluster	gainesite	$Na_2(Zr,Zn)_2(Be,Li)(PO_4)_4$	1/4
Unknown	faheyite	$(Mn,Mg,Na)Fe_2Be_2(PO_4)_4 \cdot 6H_2O$	1/2
	uralolite	$Ca_2Be_4(PO_4)_3(OH)_3 \cdot 5H_2O$	1/0.75
	glucine	$CaBe_4(PO_4)_2(OH)_4 \cdot 0.5H_2O$	1/0.5
	moraesite	$Be_2PO_4(OH) \cdot 4H_2O$	1/0.5

* Based upon BeO_4-PO_4 tetrahedral polymerization.

** Synthetic compounds reported by Harvey and Meier (1989). Note that beryllophosphate-R is essentially isostructural with pahasapaite.

1962), and the cluster structure of gainesite (Moore et al., 1983). Of these, only väyrynenite possesses a Be-P tetrahedral linkage that is not characterized by alternating Be and P tetrahedra. The väyrynenite structure contains chains of three-membered Be-Be-P tetrahedral rings linked by sharing their Be tetrahedra. Weinebeneite has gismondine-like layers of alternating Be and P tetrahedra that are joined by additional Be tetrahedra. These Be tetrahedra thereby form linked three-membered Be-Be-P tetrahedral rings similar to those in väyrynenite.

Interestingly, every natural beryllophosphate that contains the four-membered ring except beryllonite also contains Ca, and the three that do not contain four-membered rings also do not contain Ca. However, no consistent structural relationship between the Ca atoms and four-membered rings is apparent. Also, the fact that all five of the synthetic zeolite-like beryllophosphates contain four-membered rings but do not contain Ca suggests that structurally the aforementioned relationship is only coincidental. The relationship may reflect the parageneses of the beryllophosphates (see Kampf et al., 1992).

The overwhelming preponderance of linkages of tetrahedra in which Be and P tetrahedra alternate is easily explicable from Pauling bond valence considerations. Shared Be-P tetrahedral vertices yield nearly saturated O atoms, $\Sigma\ v_o = 1.75$ esu, which can approach electrostatic balance by bonding to one additional metal atom or even by accepting a H bond. Conversely, shared P-P tetrahedral vertices provide highly oversaturated O atoms with $\Sigma\ v_o = 2.5$ esu, and shared Be-Be tetrahedral vertices lead to undersaturated O atoms with $\Sigma\ v_o = 1.0$ esu. Whereas in the latter case electrostatic balance can be attained through two or more additional metal-O or H-O bonds (as in väyrynenite), the resulting bond array is more difficult to accommodate geometrically.

It is also seen that unshared P tetrahedral vertices ($\Sigma\ v_o = 1.25$ esu) are much easier to satisfy electrostatically than are unshared Be tetrahedral vertices ($\Sigma\ v_o = 0.5$ esu). In the herderite, hydroxylherderite, roscherite, zanazziite, and babefphite structures, Be tetrahedra have one shared corner, which is either an OH group or a F atom. These are the only examples of unshared Be tetrahedral vertices among the known beryllophosphate structures.

Table 9 lists all known beryllophosphate minerals and the five synthetic beryllophosphates of known structure, arranged by type of tetrahedral polymerization. Their formulas and Be/P ratios are also provided. The lowest Be/P ratio is 1/4 for the cluster-based gainesite structure. The highest is 1/0.5 for the unknown structures of glucine and moraesite. Fully condensed framework structures in which all Be and P tetrahedral vertices are shared yield a Be/P ratio of 1/1. This ratio is also found in the sheet structure of herderite, in which one Be tetrahedral vertex is unshared, and in the väyrynenite structure, in which there are shared Be-Be tetrahedral vertices. For beryllophosphate structures in which Be and P tetrahedra are strictly alternating and Be tetrahedra have at most one corner unshared by adjacent P tetrahedra, the lowest possible Be/P ratio is 1/0.75. This ratio would correspond to a structure in which all four P tetrahedral vertices are shared with Be tetrahedra but only three Be tetrahedral vertices are shared with P tetrahedra. This leads to interesting implications for the four known beryllophosphate minerals whose structures have not been solved (faheyite, glucine, moraesite, and uralolite).

When it is assumed that all Be tetrahedral vertices are shared, the faheyite structure could have chains similar to those in fransoletite, parafransoletite, and ehrleite. It is difficult, however, to reconcile the geometry of these chains with the hexagonal symmetry of faheyite. A more likely structure would be similar to that of beryllonite, with six-membered tetrahedral rings but with each P tetrahedron having two unshared vertices. Beryllonite has a pseudohexagonal cell which can be related to that of faheyite: a_f (9.43 Å) ≈ a_b/cos 30° (9.44 Å), c_f (16.00 Å) ≈ $2b_b$ (15.64 Å).

From the foregoing, uralolite, with Be/P = 1/0.75, might be expected to have a structure in which four P and three Be tetrahedral vertices are shared. This degree of condensation seems most compatible with an incomplete framework structure. Glucine and moraesite, with Be/P ratios of 1/0.5, are incompatible with structures based upon strictly alternating Be and P tetrahedra and having only one unshared B tetrahedral vertex. It seems quite likely, therefore, that Be tetrahedra share one or more vertices in the structures of these minerals as they do in the structures of väyrynenite and weinebeneite.

ACKNOWLEDGMENTS

Access to the X-ray Crystallography Laboratory of the University of California, Los Angeles, Department of Chemistry and Biochemistry was generously provided by Charles Strouse. Saeed Khan of that laboratory is acknowledged for technical assistance during data collection and analysis. Pradip K. Sen Gupta of the Memphis State University Department of Geology was very generous in providing assistance with the solution of the parafransoletite structure. Suggestions by Roland C. Rouse of the University of Michigan Department of Geological Sciences and Paul B. Moore of the University of Chicago Department of Geophysical Sciences significantly improved the manuscript.

REFERENCES CITED

Baur, W.H. (1970) Bond length variation and distorted coordination polyhedra in inorganic crystals. Transactions of the American Crystallographic Association, 6, 129–154.

Brese, N.E., and O'Keeffe, M. (1991) Bond-valence parameters for solids. Acta Crystallographica, B47, 192–197.

Brown, I.D., and Altermatt, D. (1985) Bond-valence parameters obtained from a systematic analysis of the inorganic crystal structure database. Acta Crystallographica, B41, 244–247.

Fanfani, L., Nunzi, A., Zanazzi, P.F., and Zanzari, A.R. (1975) Crystal structure of roscherite. Tschermaks mineralogische und petrographische Mitteilungen, 22, 266–277.

Fanfani, L., Zanazzi, P.F., and Zanzari, A.R. (1977) The crystal structure of a triclinic roscherite. Tschermaks mineralogische und petrographische Mitteilungen, 24, 167–178.

Giuseppetti, G., and Tadini, C. (1973) Refinement of the crystal structure of beryllonite, sodium beryllium phosphate ($NaBePO_4$). Tschermaks mineralogische und petrographische Mitteilungen, 20, 1–12.

Harvey, G., and Meier, W.M. (1989) The synthesis of beryllophosphate zeolites. In P.A. Jacobs and R.A. van Santen, Eds., Zeolites: Facts, figures, future, p. 411–420. Elsevier, Amsterdam.

Hawthorne, F.C., and Grice, J.D. (1987) The crystal structure of ehrleite, a tetrahedral sheet structure. Canadian Mineralogist, 25, 767–774.

Ibers, J.A., and Hamilton, W.C., Eds. (1974) International tables for X-ray crystallography, vol. 4. Kynoch Press, Birmingham, England.

Kampf, A.R., Dunn, P.J., and Foord, E.E. (1992) Parafransoletite, a new dimorph of fransoletite from the Tip Top Pegmatite, Custer, South Dakota. American Mineralogist, 77, 843–847.

Lager, G.A., and Gibbs, G.V. (1974) A refinement of the crystal structure of herderite, $CaBePO_4OH$. American Mineralogist, 59, 919–925.

Leavens, P.B., White, J.S., and Nelen, J.A. (1990) Zanazziite. A new mineral from Minas Gerais, Brazil. Mineralogical Record, 21, 413–417.

Lindbloom, J.T., Gibbs, G.V., and Ribbe, P.H. (1974) The crystal structure of hurlbutite: A comparison with danburite and anorthite. American Mineralogist, 59, 1267–1271.

Moore, P.B., Araki, T., Steele, I.M., Swihart, G.H., and Kampf, A.R. (1983) Gainesite, sodium zirconium beryllophosphate: A new mineral and its crystal structure. American Mineralogist, 68, 1022–1028.

Mrose, M.E., and Appleman, D.E. (1962) The crystal structures and crystal chemistry of väyrynenite, $(Mn,Fe)Be(PO_4)(OH)$, and euclase, $AlBe(SiO_4)(OH)$. Zeitschrift für Kristallographie, 117, 16–36.

Peacor, D.R., Dunn, P.J., Roberts, W.L., Campbell, T.J., and Newbury, D. (1983) Fransoletite, a new calcium beryllium phosphate from the Tip Top Pegmatite, Custer, South Dakota. Bulletin de Minéralogie, 106, 499–503.

Peacor, D.R., Rouse, R.C., and Ahn, J.-H. (1987) Crystal structure of tiptopite, a framework beryllophosphate isotypic with basic cancrinite. American Mineralogist, 72, 816–820.

Rouse, R.C., Peacor, D.R., and Merlino, S. (1989) Crystal structure of pahasapaite, a beryllophosphate mineral with a distorted zeolite rho framework. American Mineralogist, 74, 1195–1202.

Simonov, M.A., Egorov-Tismenko, Yu.K., and Belov, N.V. (1980) Use of modern X-ray equipment to solve fine problems of structural mineralogy by the example of the crystal structure of babefphite $BaBe(PO_4)F$. Soviet Physics—Crystallography, 25, 28–30.

Walter, F. (1991) Weinebeneit, ein neues Berylliumphosphat mit zeolithähnlicher Structur. Berichte der Deutschen Mineralogischen Gesellschaft, 3, 285.

MANUSCRIPT RECEIVED OCTOBER 16, 1991
MANUSCRIPT ACCEPTED FEBRUARY 25, 1992